Electronic Supplementary Information (ESI) for

Amphiphilic Janus patch-grafted hydrogel for salt-rejecting solar water desalination

Jie Zhu, Zhiyuan Xiao, Feiyu Song, Xiayun Huang, Daoyong Chen, Zhihong Nie**

The State Key Laboratory of Molecular Engineering of Polymers and Department of Macromolecular Science, Fudan University, 2005 Songhu Road, Shanghai, 200438, People's Republic of China.

**E-mail: znie@fudan.edu.cn; huangxiayun@fudan.edu.cn*

This PDF file includes:

Supplementary Text

Note S1 The quaternization degree of P4VP in 0.1 M HAc

The quaternization degree of P4VP in 0.1 M HAc (pH = 2.88) was estimated by the Henderson-Hasselbalch equation,[1]

$$a^{+} = \frac{1}{1 + 10^{pK_a - pH}} \qquad \text{(Equation S1)}$$

where the pK_a of P4VP is around 3.25.[2] Then, the quaternization degree of P4VP was calculated to be 30% in 0.1 M HAc.

Note S2 Calculation of PVA hydrogel mesh size

The mesh size (ξ) of the PVA hydrogel was calculated using the equation S2,

$$\xi = v_{2,s}^{-1/3} l \left(\frac{2C_n M_c}{M_r}\right)^{1/2} \qquad \text{(Equation S2)}$$

in which C_n = 8.3 is the Flory characteristic ratio of PVA,[3] M_r = 44.05 g/mol is the molecular weight of repeating units, l = 0.154 nm is the carbon-carbon bond length, and $v_{2,s}$ = 0.117 is the volume fraction of PVA hydrogel in the swollen state, and M_c is the number-average molecular weight between cross-links, which was calculated from the equilibrium swelling experiment using the Equation S3,[4, 5]

$$\frac{1}{M_c} = \frac{2}{M_n} - \frac{v/V[\ln(1 - v_{2,s}) + v_{2,s} + \chi v_{2,s}^2]}{v_{2,r}[(v_{2,s}/v_{2,r})^{1/3} - v_{2,s}/v_{2,r}]} \qquad \text{(Equation S3)}$$

where M_n = 88000 g/mol is the number average molecular weight of PVA, v = 0.788 cm^3/mol is the specific volume of PVA,[6] V = 18 cm^3/mol is the molar volume of the solvent, χ = 0.494 is the Flory–Huggins parameter of PVA and water,[7] and $v_{2,r}$ = 0.112 is the polymer volume fraction of PVA hydrogel in the relaxed state. Substituting the above parameters into the calculation, the mesh size of PVA hydrogel was 8 nm.

Note S3 Z-resolution of confocal microscope

The Z-resolution (R_z), the distance from the centre of the spot to the edge of the first minimum in vertical space, was estimated using Rayleigh's criterion,[8]

$$R_z = \frac{1.4\lambda\eta}{NA^2} \qquad \text{(Equation S4)}$$

in which λ is the wavelength of the excitation light, η is the refractive index of the mounting medium (speed at which light propagates through the material), and NA is the numerical aperture of objective lens.[9] In our system, the wavelength of the excitation light was 550 nm. The reflective index of the medium (η) and the numerical aperture of the lens (*NA*) was 1.33 and 0.8 for 40x water immersion objective lens. Thus, the Z-resolution was calculated to be 2 μm. Therefore, the smallest depth observed is 4 μm.

Note S4 Statistics on nearest-micelle distance

The nearest-micelle distance was defined as the minimum distance between adjacent disperse micelles, which was used to quantify the uniformity of the micelles that grafted to the PVA hydrogels.[10] First, the barycentric coordinates (x_p, y_p) of each micelle on the micelle-grafted PVAs were measured using the Analyze Particles tool in Fiji software. Then, the centre-to-centre micelle distances and their distributions were calculated based on the collected barycentric coordinates using the program written by us. Moreover, the micelle grafting density (cm^{-2}) was also measured using the Analyze Particles tool in Fiji software.

Note S5 Calculation of efficiency of PVA, SVJ-1 and SVQJ-1

The evaporation efficiency (η, %) of water, PVA, SVJ-1 and SVQJ-1 was calculated by the equation S5,

$$\eta = \frac{r \times E_{equ}}{q_{solar}} \quad \text{(Equation S5)}$$

where r was the evaporation rate (kg m^{-2} h^{-1}) after reaching the steady evaporation state, E_{equ} was the equivalent enthalpy (J/g) obtained by the dark experiment, q_{solar} was the solar flux (kW m^{-2}).[11] The initial ambient temperature and the humidity of the surroundings in the dark experiment were fixed at 20°C and 45%, respectively. In the dark experiment, the E_{equ} can be estimated by vaporizing water with identical power input, which has the relationship shown in the equation S6,

$$E_0 \times M = E_{equ} \quad \text{(Equation S6)}$$

where E_0 is the evaporation enthalpy (J/g) of water and M is the ratio of mass change of bulk water over evaporators. Based on the above equations, the measured equivalent enthalpy and calculated efficiency of water were 2390 J/g and 21%, which were very close to the reference values (2450 J/g and 20%),[12] confirming the accuracy of our measurements and calculations.

Supplementary Figures

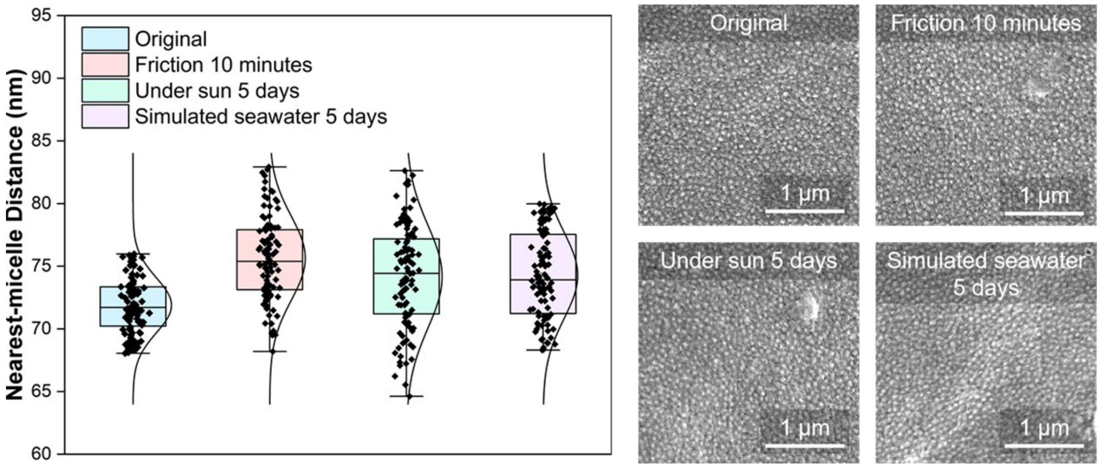

Fig. S1 The nearest-micelle distance of SVQ-1-60 after being exposed to the various durable operation conditions, including friction for 10 min (1 N, 40 Hz), under sun for 5 days, immersed in simulated seawater for 5 days, and the corresponding SEM images. The average nearest-micelle distance exhibited the deviations of no more than 5 nm from the original value, indicating the stable entanglement between quaternized P4VP and the hydrogel.

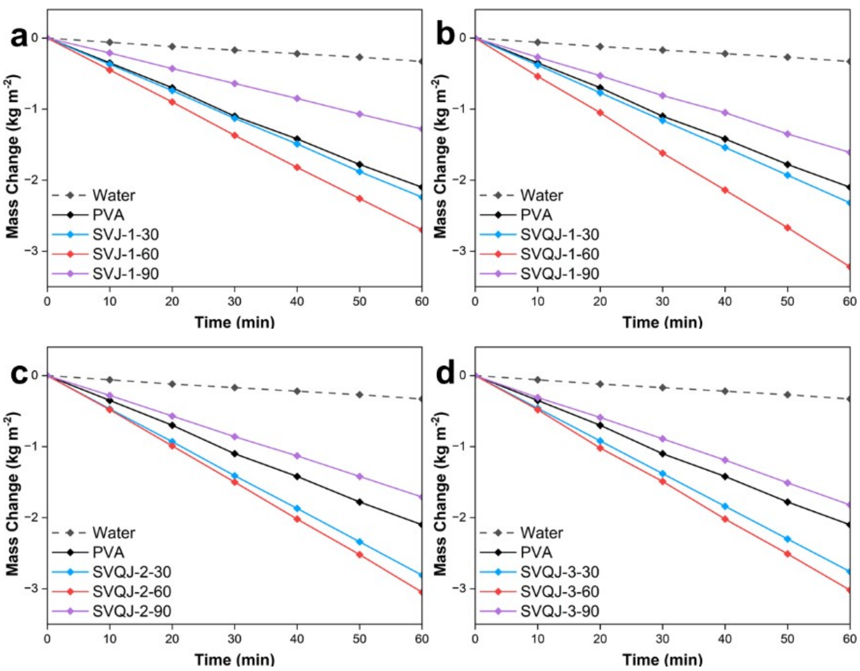

Fig. S2 Evaporation curves of water, PVA hydrogel, (a) SVJ-1, (b) SVQJ-1, (c) SVQJ-2, and (d) SVQJ-3 hydrogels prepared at different grafting time.

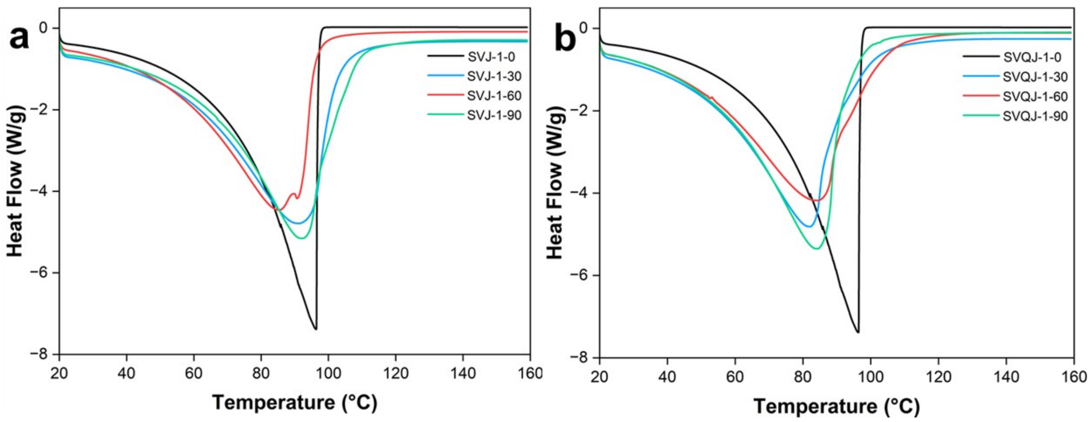

Fig. S3 Heat flow of SVJ-1 and SVQJ-1 prepared at different grafting time from 20^{o}C to 160^{o}C, analyzed by DSC. The corresponding evaporation enthalpy was shown in **Fig. 3d**.

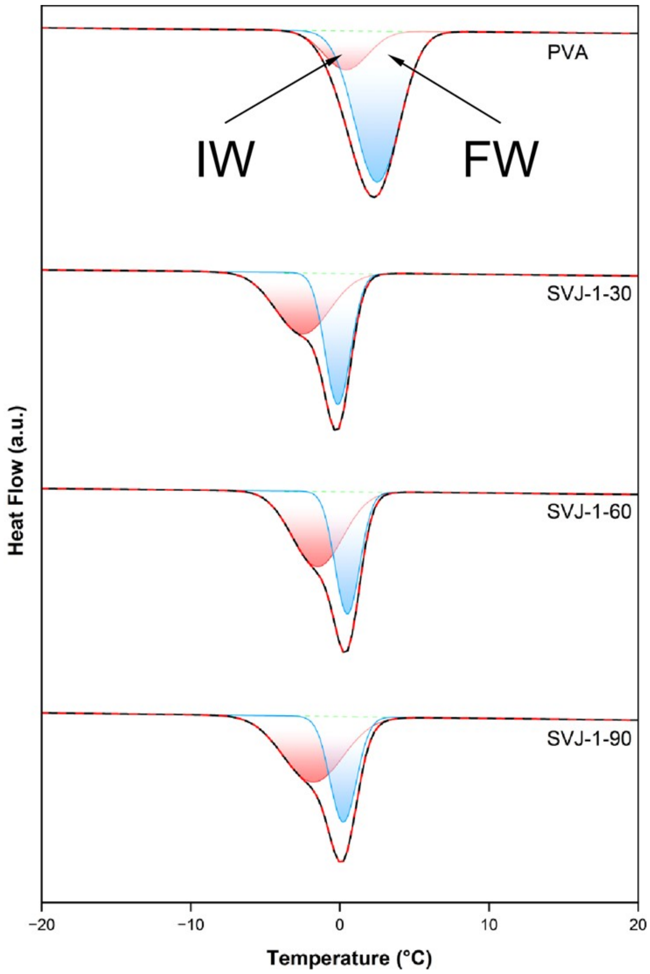

Fig. S4 Heat flow of SVJ-1 prepared at different grafting time analyzed by DSC. The corresponding IW/FW ratio was shown in **Fig. 3e**. Hydrogel samples were soaked in DI water for 24 hours to become fully swollen before DSC measurements. For the DSC measurement, the hydrogel was tightly sealed in an aluminum crucible to prevent water evaporation and maintained at -30 °C for 5 minutes to be fully frozen. The measurement was then performed with scans at a linear heating rate of 2 °C/min under a nitrogen flow rate of 50 mL/min, within a temperature range from -30 °C to 30 °C. As the temperature increased, the peaks located near 0 °C correspond to the melting of intermediate water and free water, respectively. The Gaussian function was used to fit the two peaks corresponding to FW and IW, respectively, and the IW/FW ratio was calculated based on the integral areas of IW and FW.

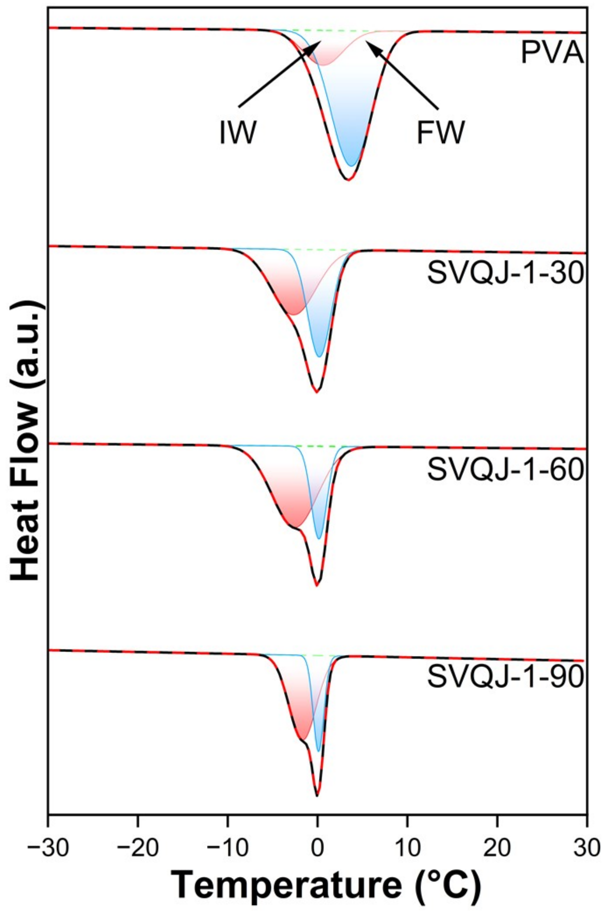

Fig. S5 Heat flow of SVQJ-1 prepared at different grafting time analyzed by DSC. The corresponding IW/FW ratio was shown in **Fig. 3e**.

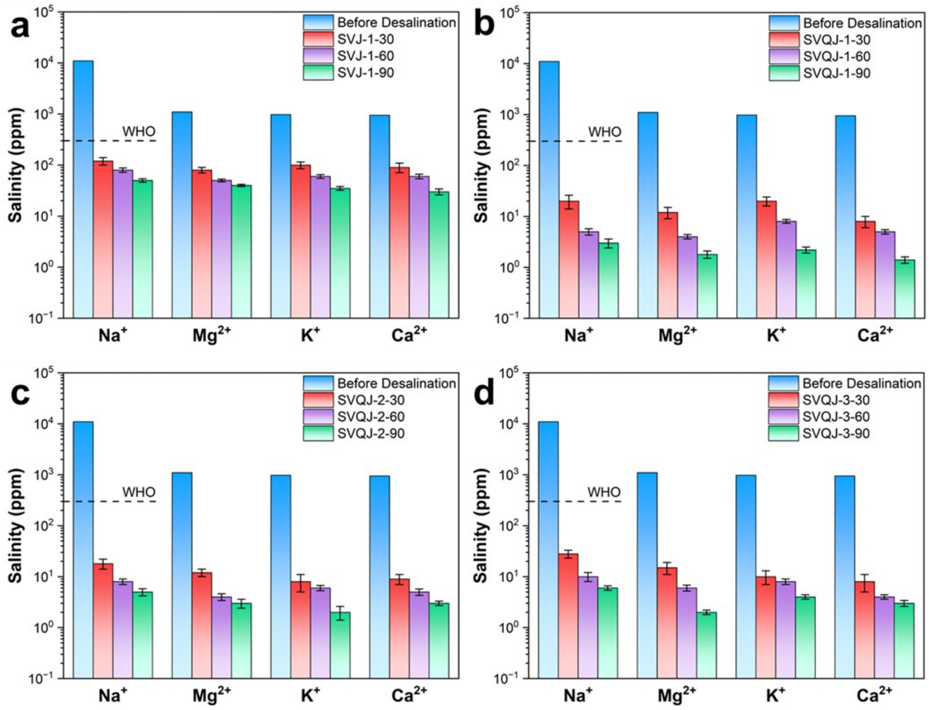

Fig. S6 Ion concentrations in the simulated seawater and condensed water after the desalination using (a) SVJ-1, (b) SVQJ-1, (c) SVQJ-2, and (d) SVQJ-3 hydrogels prepared at different grafting time. The concentrations of cations in the simulated water, including sodium ion (Na^+), magnesium ion (Mg^{2+}), potassium ion (K^+), and calcium ion (Ca^{2+}), in both the original simulated seawater and the desalinated water were measured using ICP-MS. The concentrations were summed separately and denoted as C_0 and C_1. The "ion rejection ratio" is defined as $(C_0 - C_1) / C_0 \times 100\%$. The 'ion rejection ratio' is used in this work to evaluate the salt resistance capacity of various solar evaporators, shown in **Fig. 3f** and **Fig. 4g, h**.

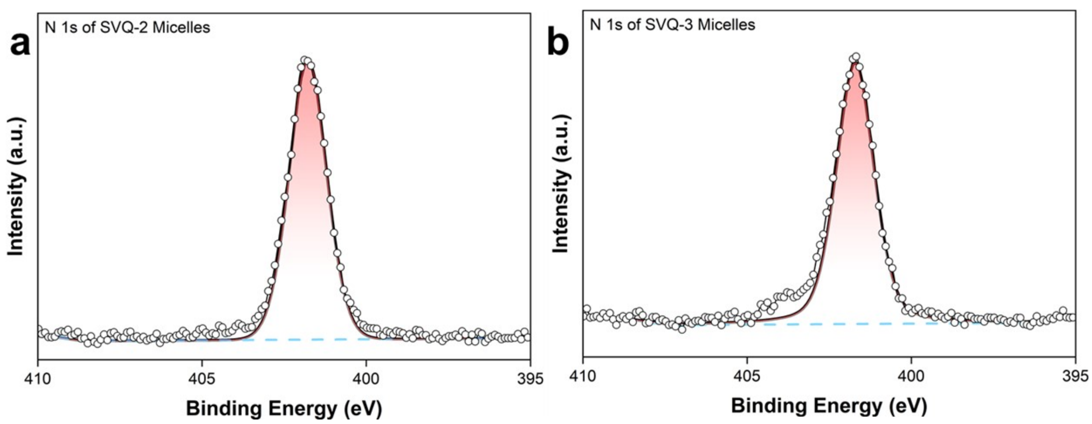

Fig. S7 N 1s XPS spectra of SVQ-2 and SVQ-3 micelles.

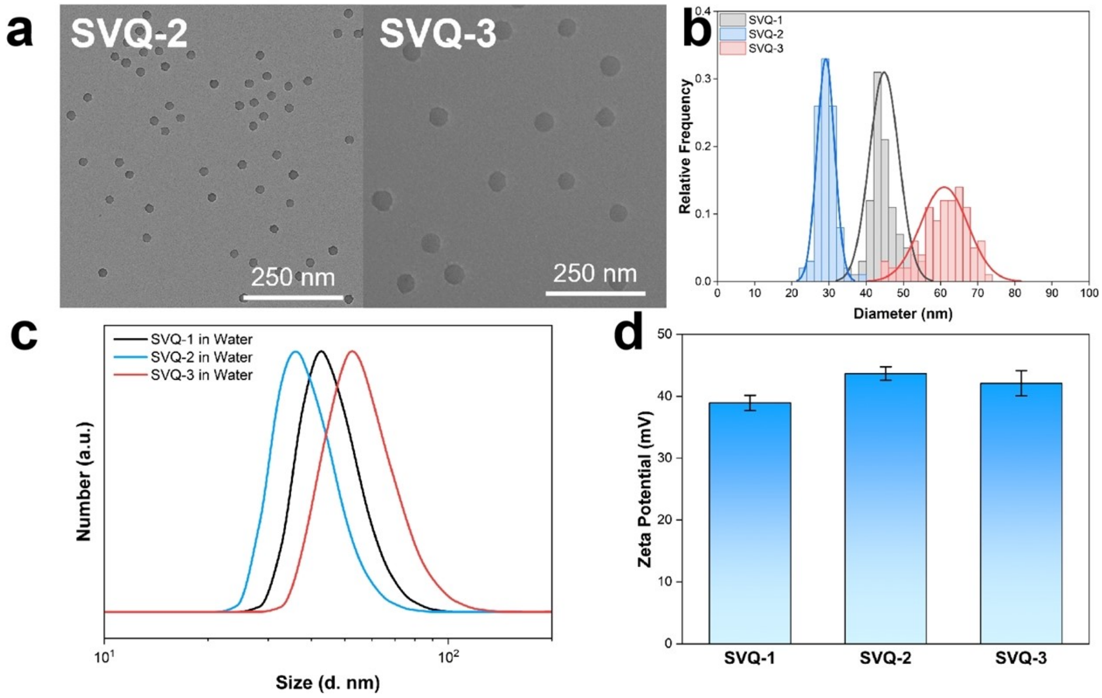

Fig. S8 (a) TEM images of SVQ-2 and SVQ-3 micelles. (b) The histogram of the diameter of SVQ-1, SVQ-2, and SVQ-3 micelles. (c) DLS traces and (d) zeta potentials of SVQ-1, SVQ-2, and SVQ-3 micelles.

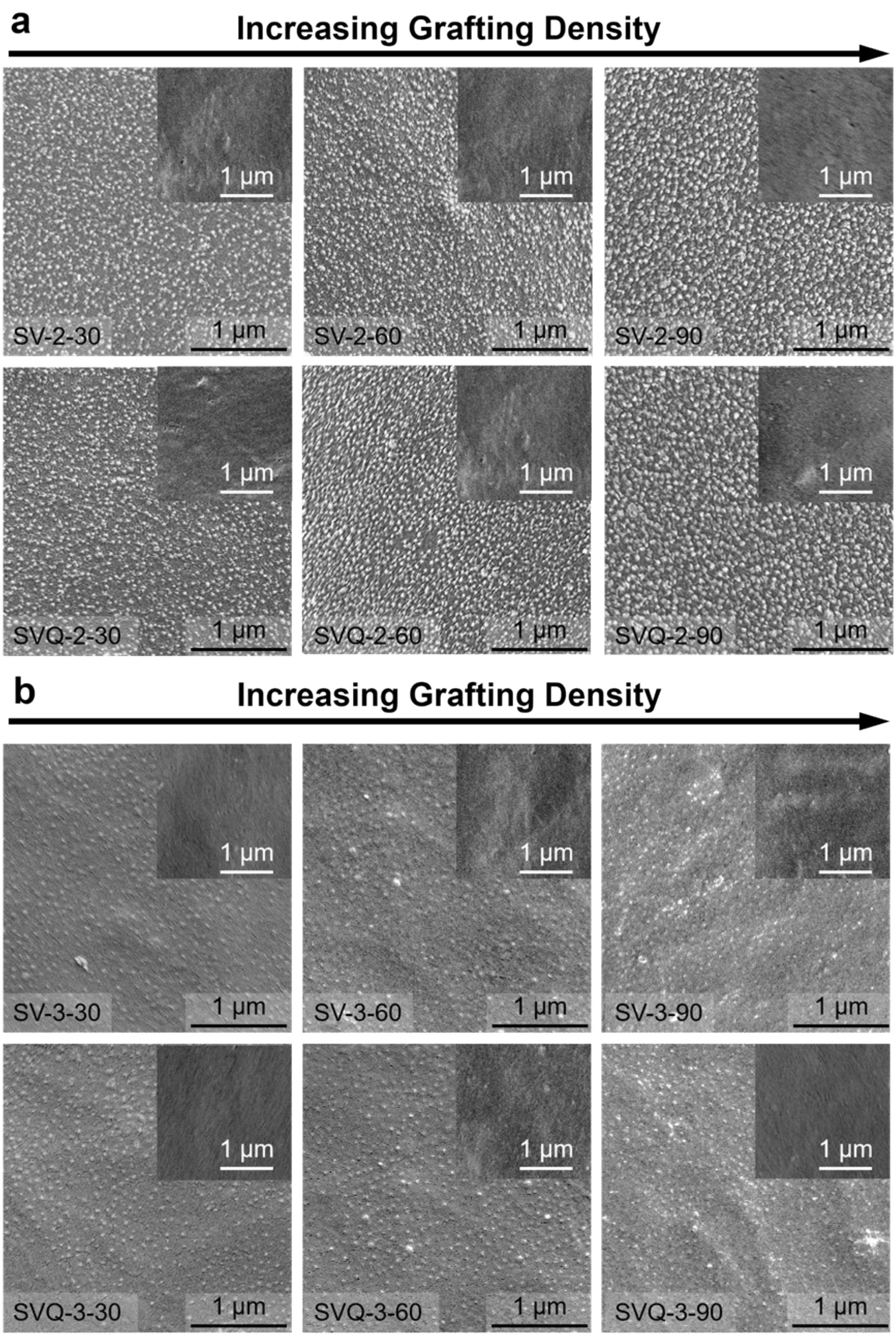

Fig. S9 (a) SEM images of electric-field grafting SV-2 micelles and SVQ-2 micelles on PVA hydrogel for 30, 60, and 90 min. (b) SEM images of electric-field grafting SV-3 micelles and SVQ-3 micelles on PVA hydrogel for 30, 60, and 90 min. Inserted images are the corresponding samples after solvent wash.

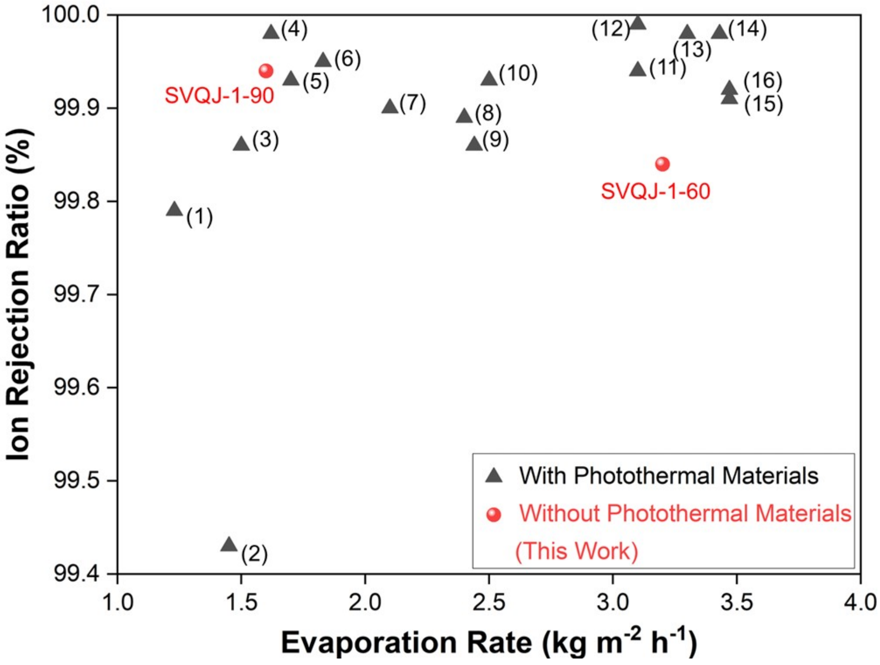

Fig. S10 Water evaporation rate *versus* ion rejection ratio for reported 2D solar water evaporators under one sun irradiation.

Supplementary Tables

Table S1 A summary of water evaporation rate, ion rejection ratio of a series reported 2D solar water evaporators under one sun irradiation.

No.	Hydrogel substrate	Photothermal material	Evaporation rate (kg m^{-2} h^{-1})	Ion rejection ratio (%)	Ref.
1	AlgCa	PEDOT:PSS	1.2	99.79	13
2	AlgAl	rGO	1.4	99.43	14
3	PAA/CNC	Metallic sulfides	1.5	99.86	15
4	P(SBMA-*co*-METAC)	PPy	1.6	99.98	16
5	PEG/Chitosan	Mars black paint	1.7	99.93	17
6	Lignocellulose	Lignin-derived carbon	1.8	99.95	18
7	Corn starch	Activated carbon	2.1	99.90	19
8	P(AAm-co-AA)	Carbon black	2.4	99.89	20
9	PAAm/PDEAAm	CuS	2.4	99.86	21
10	PVA/PAAm	CNT	2.5	99.93	22
11	PVA	Aramid nanofibers/PPy	3.1	99.94	23
12	PVA/Konjac glucomannan	Fe-MOF	3.1	99.99	24
13	PAAm	MoS_2	3.3	99.98	25
14	PVA/PSS	Activated carbon/Fe_3O_4	3.4	99.98	26
15	PVA/PEI	CB/CNT	3.5	99.91	27
16	PVA	Liquid metal/Ag nanowires	3.5	99.92	28
17	**SVQJ-1-90**	**None**	**1.6**	**99.94**	**This Work**
	SVQJ-1-60	**None**	**3.2**	**99.84**	

References

1. D. G. Mintis and V. G. Mavrantzas, *J. Phys. Chem. B*, 2019, **123**, 4204-4219.
2. A. San Juan, D. Letourneur and V. A. Izumrudov, *Bioconjugate Chem.*, 2007, **18**, 922-928.
3. L. F. Gudeman and N. A. Peppas, *J. Appl. Polym. Sci.*, 1995, **55**, 919-928.
4. N. A. Peppas and S. L. Wright, *Macromolecules*, 1996, **29**, 8798-8804.
5. N. A. Peppas and E. W. Merrill, *J. Appl. Polym. Sci.*, 1977, **21**, 1763-1770.
6. W. Ma, P. Zhang, B. Zhao, S. Wang, J. Zhong, Z. Cao, C. Liu, F. Gong and H. Matsuyama, *J. Polym. Sci. Pol. Phys.*, 2019, **57**, 1673-1683.
7. H. Matsuyama, M. Teramoto and H. Urano, *J. Membr. Sci.*, 1997, **126**, 151-160.
8. J. Jonkman, C. M. Brown, G. D. Wright, K. I. Anderson and A. J. North, *Nat. Protoc.*, 2020, **15**, 1585-1611.
9. A. D. Elliott, *Curr. Protoc. Cytom.*, 2020, **92**, e68.
10. Z. Xu, J. M. Seddon, P. A. Beales, M. Rappolt and A. I. I. Tyler, *J. Am. Chem. Soc.*, 2021, **143**, 16556-16565.
11. Y. Guo, X. Zhao, F. Zhao, Z. Jiao, X. Zhou and G. Yu, *Energy Environ. Sci.*, 2020, **13**, 2087-2095.
12. J. Ren, L. Chen, J. Gong, J. Qu and R. Niu, *Chem. Eng. J.*, 2023, **458**, 141511.
13. X. Zhao and C. Liu, *Desalination*, 2020, **482**, 114385.
14. X. Hao, H. Yao, P. Zhang, Q. Liao, K. Zhu, J. Chang, H. Cheng, J. Yuan and L. Qu, *Nat. Water*, 2023, **1**, 982-991.
15. M. Li, B. Liu, Z. Liu, Y. Xiao, H. Guo, Z. An, L. Wang and T. D. James, *Adv. Funct. Mater.*, 2023, **33**, 2209987.
16. B. Peng, Q. Lyu, Y. Gao, M. Li, G. Xie, Z. Xie, H. Zhang, J. Ren, J. Zhu, L. Zhang and P. Wang, *ACS Appl. Mater. Interfaces*, 2022, **14**, 16546-16557.
17. Y. Liu, Y. Tian, N. Liu, S. Zhao, H. Zhai, J. Ji, W. Cao, L. Tao, Y. Wei and L. Feng, *Small*, 2024, **20**, 2305903.
18. X. Lin, P. Wang, R. Hong, X. Zhu, Y. Liu, X. Pan, X. Qiu and Y. Qin, *Adv. Funct. Mater.*, 2022, **32**, 2209262.
19. S. Zhang, M. Li, C. R. Jiang, D. D. Zhu and Z. H. Zhang, *Adv. Sci.*, 2024, 2308665.
20. Y. Liang, Y. Bai, A. Xie, J. Mao, L. Zhu and S. Chen, *Sol. RRL*, 2022, **6**, 2100917.
21. J. Chen, A. Chu, H. Yang, J. Zhao, M. Yang, J. Fang, Z. Yang, Z. Wang and H. Li, *Sol. RRL*, 2024, **8**, 2300649.
22. J. Zhou, Z. Sun, X. Mu, J. Zhang, P. Wang, Y. Chen, X. Wang, J. Gao, L. Miao and L. Sun, *Desalination*, 2022, **537**, 115872.
23. H. Li, W. Zhang, J. Liu, M. Sun, L. Wang and L. Xu, *Adv. Funct. Mater.*, 2023, **33**, 2308492.

24. Y. Guo, H. Lu, F. Zhao, X. Zhou, W. Shi and G. Yu, *Adv. Mater.*, 2020, **32**, 1907061.
25. P. Liu, Y. Hu, X. Li, L. Xu, C. Chen, B. Yuan and M. Fu, *Angew. Chem. Int. Ed.*, 2022, **61**, e202208587.
26. B. Wang, K. Yang, B. Cai, J. Zhang, C. Wei and A. Zhou, *Chem. Eng. J.*, 2023, **465**, 142944.
27. L. Zhao, Z. Yang, J. Wang, Y. Zhou, P. Cao, J. Zhang, P. Yuan, Y. Zhang and Q. Li, *Chem. Eng. J.*, 2023, **451**, 138676.
28. S. Yang, Y. He, J. Bai and J. Zhang, *Small*, 2023, **19**, 2302526.